# High-pressure melting curve of helium and neon: Deviations from corresponding states theory

David Santamaría-Pérez,[1,2] Goutam Dev Mukherjee,[1,3,*] Beate Schwager,[1] and Reinhard Boehler[1,4]
[1]*Max Planck Institut für Chemie, Postfach 3060, D-55020 Mainz, Germany*
[2]*Departamento de Química Física I–MALTA Consolider Team, Universidad Complutense de Madrid, Avda. Complutense s/n, 28040 Madrid, Spain*
[3]*Physics Department, Indian Institute of Science Education and Research Kolkata, P.O. BCKVV Campus Main Office, Nadia, 741252 West Bengal, India*
[4]*Geophysical Laboratory, Carnegie Institution of Washington, 5251 Broad Branch Road NW, Washington, D.C. 20015, USA*
(Received 28 October 2009; revised manuscript received 10 February 2010; published 2 June 2010)

The melting curves of He and Ne were measured up to 80 and 70 GPa, respectively, significantly extending the pressure range of previous measurements. Melting was detected *in situ* by the laser speckle method using the laser-heated diamond-anvil cell. Temperatures were measured in the visible as well as infrared range. Our He melting curve differs considerably from earlier experimental data above 30 GPa. The present Ne melting curve does not agree with the predictions from corresponding states theory in the range from 15 to 70 GPa.

DOI: 10.1103/PhysRevB.81.214101 PACS number(s): 64.70.dj, 62.50.−p

## I. INTRODUCTION

The melting curves of the rare gas solids He, Ne, Ar, Kr, and Xe are of fundamental interest as a test case for theoretical melting models and because they are frequently used as pressure transmitting media in laser-heated diamond-anvil cell (LHDAC) experiments. Recent melting experiments on the heavier rare gas solids,[1–6] Ar, Kr, and Xe showed a significant flattening in the melting curves at high pressure (near 40, 30, and 20 GPa for Ar, Kr, and Xe, respectively),[5,6] in stark contrast to theoretical predictions based on corresponding states. This melting behavior is most likely due to a peculiar behavior in their structural properties: it was shown that for these rare gas solids the transition from the fcc to the hcp phase has a very large pressure range,[2,3,7] and the bend in the melting slopes of the heavier rare gas solids has been attributed to effects of hybridization of the *p*-valence states and *d*-conduction states due to band gap narrowing at high pressures.[6] Earlier theoretical studies have suggested that the stabilization of the hcp-phase in these rare gas solids is due to such a hybridization process.[4]

Helium, the first member of the rare gas family, has been studied extensively.[8–20] At ambient pressure He crystallizes in the hcp structure at 0.95 K. Early specific heat measurements on He showed the existence of an hcp-fcc phase transition at $P > 1.12$ kbar, with the hcp-fcc-liquid triple point placed at 0.11 GPa and 15 K.[8] Melting experiments on He using a diamond anvil cell (DAC) showed a small cusp at 11.6 GPa and 299 K that pointed to the existence of a triple point and a new high pressure phase.[12] Single crystal x-ray diffraction measurements on He up to 58 GPa showed the new phase to be hcp.[16]

The melting curve of helium has been experimentally determined up to 24 GPa by Vos *et al.*,[17] and up to 41 GPa by Datchi *et al.*[19] using the quasi-isochoric scanning method. Their results are in good agreement up to 19 GPa and 400 K, where the measured melting temperatures start to deviate slightly. However, the extrapolation of the fitted curves in these studies gives a temperature difference of 200 K (about 20%) at a pressure of 80 GPa. Recent molecular dynamic calculations[20] reproduced very well the experimental melting curve of Vos *et al.* up to 23 GPa.

Neon, the second member of the rare gas family, crystallizes to an fcc solid at 24.4 K at ambient pressure. Early high-pressure experiments have shown that fluid neon freezes to the above solid at about 4.7 GPa at room temperature.[21,22] Recent high-pressure x-ray diffraction studies on neon up to 110 GPa at room temperature do not show any structural transition.[23] The electronic structure of neon is also expected to behave differently from those of the heavier rare gas solids as the energy band gap between the filled $2p$-valence states to the $3d$-conduction state is quite large. Therefore, the physical properties of Ne including its melting behavior at extreme pressures may turn out to be different from the other heavy rare gas solids. In contrast to He, the melting curve of neon was experimentally determined only up to 5.5 GPa and 328 K using an externally heated diamond anvil cell.[9,24] The melting curve of Ne at high pressures was predicted by Datchi *et al.*[19] by applying the law of corresponding states principle to the experimentally observed melting curve of He up to 44 GPa. It was shown that the predicted Ne melting curve agrees well with the calculations based on the exponential-6 potential[24] and does not show any anomalous behavior.

In this paper, we report new measurements of the melting curve of He and Ne up to 80 and 70 GPa, respectively, using the LHDAC technique. These measurements show that the new melting curves do not agree with the previous theoretical calculations as well as the law of corresponding states.

## II. EXPERIMENTAL

For the He experiments, diamond-cell used was of the Boehler-Almax type[25] and for Ne standard piston-cylinder type diamond cells were used with conical diamond anvils having 270–300 $\mu$m culets. Tungsten disks of 4–8 $\mu$m thickness were used as absorbers for the IR laser in the LH-DAC. The tungsten disks were made by pressing small grains (of 99.9+% purity from Aldrich, Prod. Nr. 267511) between the flat culets of two diamonds. The absorber disks

 

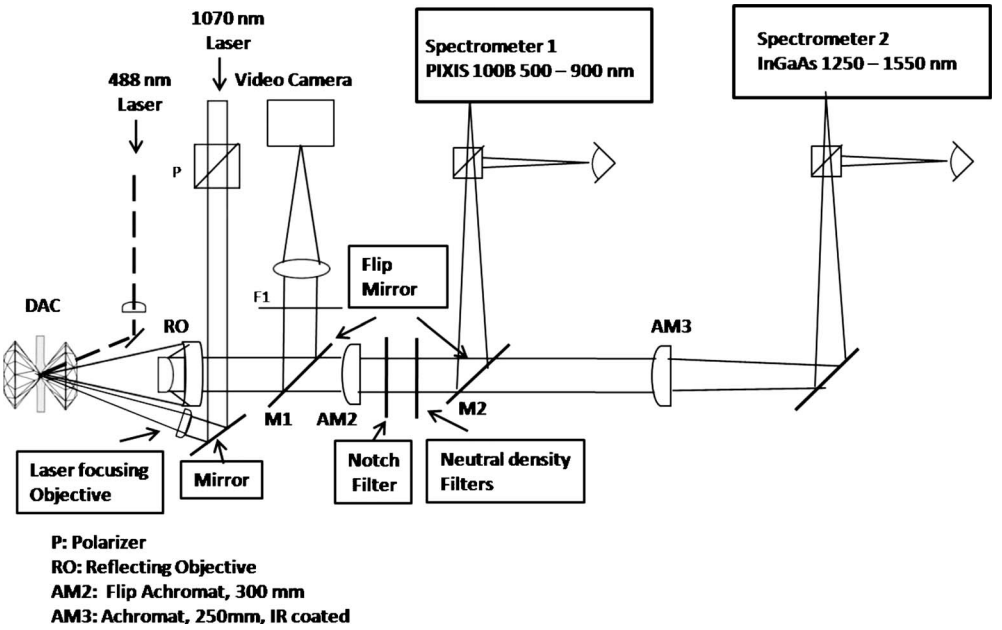


FIG. 1. Schematics of the experimental setup used for the melting studies of He and Ne. The flip mirror M1 is used to observe the laser speckle using an argon laser (488 nm). For temperature measurement using spectrometer 1 with PIXIS 100B CCD, M1 is removed. For measurements using Spectrometer 2 with InGaAs CCD, AM2, and M2 are moved away.

were placed at the center of the 80–110 $\mu$m diameter hole of tungsten gasket, preindented to a thickness of 40–50 $\mu$m. For the He experiments the diamonds were coated with $Al_2O_3$ in order to thermally insulate the heater from the diamonds and to reduce diffusion of He into the diamonds at high pressures. The coating with a thickness of about 300 nm was applied after preindenting the tungsten gasket to a thickness of 40 $\mu$m, using an etching/sputtering machine (Gatan Inc., PECS, model 682). He and Ne gas of 99.99% purity were loaded in the LHDAC at room temperature using the 0.3 GPa gas loading apparatus. Ruby chips for pressure measurement were evenly distributed close to the W heater. Pressures were measured before and after heating by the ruby fluorescence method.[26] A diode pumped YLR-100-SM series (IPG Photonics Corporation, USA) single mode cw ytterbium fiber laser (maximum power of 100 W) at the wavelength of 1.07 $\mu$m was used to heat the tungsten absorber. The laser beam was defocused in order to obtain a large hot spot with uniform temperature within an area with approximately 20 $\mu$m in diameter. Initially, in each run, the laser power was increased until a visible hotspot was created ($T \approx 1400$ K) in order to align the center of the hotspot with the entrance pinhole of the spectrometer. A schematic sketch of the experimental configuration, which was used to record the incandescent light emitted from the hot sample in two different wavelength ranges: 1250–1550 nm (for He) and 500–900 nm (for both He and Ne) is given in Fig. 1. For temperature measurements, incandescent light from an area of 2 $\mu$m at the center of the hot spot was collected by an aberration-free-reflecting objective (see Fig. 1) and detected with spectrometers in the two different spectral ranges: (a) in 1250–1550 nm with a liquid nitrogen cooled InGaAs detector (2D-OMA V, Princeton Instruments) and (b) in 500–900 nm with a thermoelectrically cooled back-illuminated deep-depleted charge-coupled device (CCD) (Pixis Model 100 B, Princeton Instruments). This temperature measurement system was calibrated with a tungsten filament light source with-known intensity versus wavelength distribution. This method was checked against a calibrated blackbody source of our own design. At 750 K, the temperature difference between the radiometric method and the blackbody is of the order of $\pm 10$ K for both spectrometers.

Planck's radiation function,

$$I(\lambda) = \frac{\epsilon C_1 \lambda^{-5}}{e^{C_2/\lambda T} - 1}, \tag{1}$$

was then fitted to the collected spectrum, where $I$ is the intensity of the spectrum and $C_1$ and $C_2$ are constants. Fitting was carried out with the emissivity $\epsilon$ and the temperature $T$ as free parameters, assuming constant emissivity as a function of wavelength across the recorded spectral range. A blue laser (488 nm line of Ar-ion laser) was focused on the sample (Fig. 1), which created an interference pattern on the surface of the absorber, made visible with a video camera. When the surface of the tungsten absorber reached the melting temperature of the rare gas solid, a thin layer of liquid formed in contact with the heated absorber surface. Temperature gradients inside the cell produced rapid convection of the liquid layer creating local changes in the refractive index and showing up as a continuous rapid motion of the interference pattern of the heating laser. At increasing laser power the onset of continuous motion, due to molten gas, occurs over a very narrow temperature interval and, equally, the cessation of motion at freezing. Temperatures were measured at the onset of the laser speckle motion (melting) while increasing the laser power and at the disappearance of the motion (freezing) while decreasing the laser power. The re-

ported melting temperatures are the mean value of temperatures measured for five melting and freezing cycles showing maximum deviations within ±100 K. After each experiment, the tungsten absorber was visually inspected to check for signs of any chemical reaction. The above laser speckle method for melting experiments in the LHDAC has been used extensively and provided accurate results for other heavier noble gas solids,[5] alkali halides,[27] and nitrogen.[28] Very recently we verified melting temperatures of Mo and Fe obtained previously using the laser speckle method with new x-ray diffraction measurements at over 100 GPa.[29]

One notable observation was that during melting, tungsten absorbers with very small dimensions moved around inside the gasket hole even above 40 GPa. For Ne, above 55 GPa the laser speckle motion gradually slowed down restricting our melting curve measurement to about 70 GPa. The cause of this observation is not entirely clear. It could be due to the small volume change at melting, the change in surface tension, or the change in viscosity or any combination of those. To check the consistency of Ne melting data we used both loosely packed Ir-black powder and diamond in place of tungsten absorbers to observe Ne melting. The diamond heaters were laser cut from nanocrystalline chemical vapor deposition (CVD) diamond with a thickness of 12–13 $\mu$m and diameter of about 60–50 $\mu$m with a central hole with about 5 $\mu$m in diameter. These diamond plates heated very uniformly with a perfect circular glow and the laser speckle pattern was observed near the central hole. However, since Ne is highly compressible, we could not reach very high pressures as the top anvil started touching the diamond heater. For Ir pellets as absorber we could observe the laser speckle motion only at lower pressures.

## III. RESULTS AND DISCUSSION

In Fig. 2, we present our melting data on He together with previous melting results obtained in a large volume multi anvil apparatus up to 2 GPa[9,11] and in externally heated diamond anvil cell up to 41 GPa.[17,19] We have also included for comparison the theoretical melting curve of He reported by Koči *et al.*[20] and Loubeyre and Hansen[14] from molecular dynamics calculations. The measured melting temperatures increase continuously with pressure in the whole pressure range studied. From the Fig. 2, it can be seen that our results are close to the melting curve predicted by Vos *et al.*,[17] who used a Simon-Glatzel (SG) equation[30] to extrapolate their data (dotted line in Fig. 2). Our experimental He melting curve lies only slightly above this curve. Fitting the SG equation to our He experimental data, however, did not reproduce the low pressure melting curves reported in literature.[9,17] Therefore, we fitted a Kechin equation[31] to our He melting data

$$T_m(K) = T_0\left[1 + \frac{\Delta P}{a}\right]^b e^{c\Delta P}, \qquad (2)$$

yielding $a=0.09(3)$, $b=0.61(5)$, and $c=0.002(1)$, where $P=P-P_0$ with $P_0=0.1135$ GPa and $T_0=15.06$ K are the coordinates of the first triple point of He (hcp-fcc-liquid).

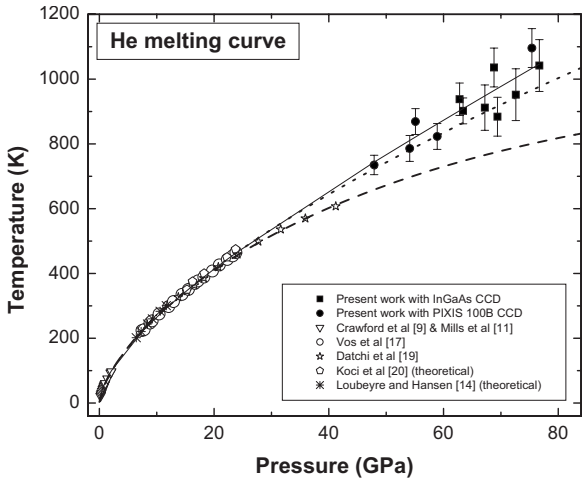


FIG. 2. Melting curve of He. The present data is represented by (a) filled squares (taken with InGaAs CCD in the infrared range); (b) filled circles (taken with PIXIS 100B CCD in the visible range). Previous experimental data are represented by (a) triangles (Refs. 9 and 11), (b) open circles (Ref. 17), and (c) stars (Ref. 19). Dotted and dashed lines represent the fittings to the Simon-Glatzel equation reported by Vos *et al.* (Ref. 17) and the Kechin equation reported by Datchi *et al.* (Ref. 19), respectively. Kechin equation fit to the present data is represented as a solid line. The theoretical melting points reported by (a) Loubeyre and Hansen (Ref. 14) are given by crosses and (b) Koči *et al.* (Ref. 20) given by pentagons.

In Fig. 2, we compare our LHDAC results for He with those of externally heated DAC measurements from Crawford and Daniels,[9] Mills *et al.*,[11] Vos *et al.*,[17] and Datchi *et al.*[19] The extrapolation of our data to low pressures yield the melting curve represented by the solid line, which agrees well with the earlier experimental data and theoretical predictions up to about 30 GPa reported in literature.[9,11,14,17,20] This melting curve is in good agreement with the extrapolated melting curve by Vos *et al.*[17] The experimental data reported by Datchi *et al.*[19] start to deviate from our melting curve above about 30 GPa. A closer look in the Fig. 5 of the paper of Datchi *et al.*[19] shows a clear deviation of melting data starting from 20 GPa with respect to the work of Vos *et al.*[17] The difference between our data and the work of Datchi *et al.*[19] may be explained by the method of temperature measurement of Datchi *et al.* Temperatures were measured indirectly by the shift of the ruby fluorescence $R1$ line[19] and this shift is both pressure and temperature dependent and not well calibrated at high $P$-$T$ conditions.

In Fig. 3, we show the results of the present Ne melting measurements up to 70 GPa, using three different starting conditions: (i) tungsten absorbers of 4–8 $\mu m$ thickness (open symbols), (ii) loosely pressed pellet of very fine iridium-black powder (filled triangles), and (iii) diamond heaters (filled pentagons). We observed some difference in melting temperatures depending on the starting conditions, but the scatters in our melting data points lie within a band of uncertainty of 200 K. A Simon-Glatzel fit to our experimental melting data yielded

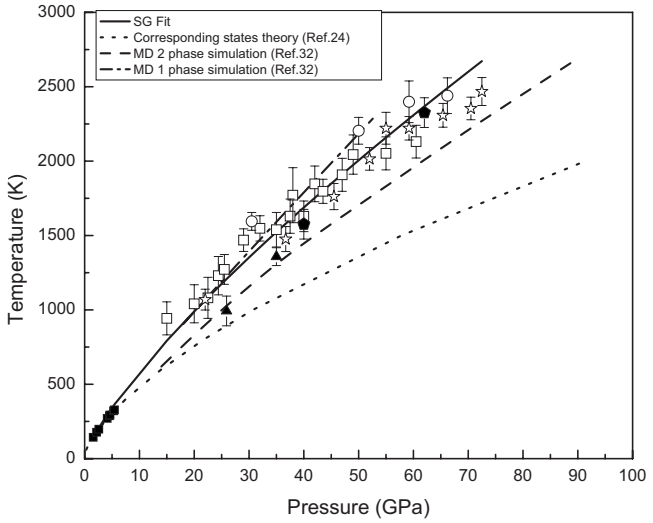


FIG. 3. Melting curve of neon. The open symbols belong to melting data points using W absorbers of different thickness: (a) open squares represent thickness of about 8 micron; (b) open circles represent thickness of about 4–6 micron; (c) open stars represent thickness of about 6–8 $\mu$m. Filled pentagons are data points obtained using diamond heaters and filled triangles represent loosely packed Ir black absorbers. The low pressure melting data represented by filled squares are taken from Vos *et al.* (Ref. 24).

$$T_m(K) = T_0\left[1 + \frac{\Delta P}{0.17}\right]^{0.77}, \tag{3}$$

where $T_m$ is the melting temperature, $\Delta P = P - P_0$, and $T_0$(=24.4 K) is the melting temperature of Ne at atmospheric pressure $P_0$. The largest deviations of the experimental data from this curve are within $\pm 200$ K and all our data lay within that band. As shown in the Fig. 3, extrapolation of this fit to lower pressures yields good agreement with the low pressure melting data points (Vos *et al.*[24]). In the same figure we have included the melting curve calculated by the principle of corresponding states using the depth and location of the exponential-6 potential energy minimum to scale the melting curve of Ar to Ne.[24] We have also included for comparison the theoretical melting curve of Ne recently reported by Koči *et al.*[32] from first-principles and classical one- and two-phase molecular dynamics simulations.

The large pressure-temperature range of the new helium melting curve provides an excellent test to verify the validity and the extension of the law of corresponding states for melting curve determination of other noble gases at very high pressures. This law states that the rare gas solids can be described by the same form of intermolecular potential and should have the same reduced form of the equation of state. High-pressure properties of noble gas solids are well-described by an exponential-6 potential with a stiffness parameter ($\alpha$) between 13 and 13.2.[19] In this way, the pressure and the temperature at melting ($P_m, T_m$) of any noble gas could be scaled from the $P_m$ and $T_m$ of other noble gas, knowing the energy ($\epsilon$) and the position ($r^*$) of the minimum wells. These parameters are $\epsilon = 10.8$, 42, 122, and 235 K and $r^* = 2.967$, 3.18, 3.85, and 4.47, respectively, for He, Ne, Ar, and Xe.[19,20] The expressions to scale the pressure and the temperature are

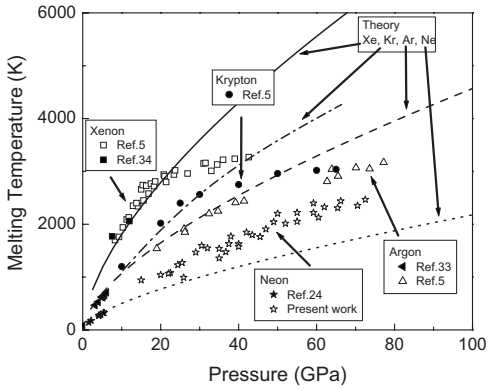


FIG. 4. Dotted, dashed, dot-dash and solid lines represent the predicted melting curves of Ne, Ar, Kr, and Xe obtained by corresponding states scaling from our He melting curve. To compare, the solid points corresponding to experimental melting data: filled stars (Ref. 24) and open stars (present work) for Ne; filled triangles (Ref. 33) and open triangles (Ref. 5) for Ar, filled circles for Kr (Ref. 5) and open squares (Ref. 5) and filled squares (Ref. 34) for Xe.

$$P(X) = P(Y)\left\{\frac{\epsilon(X)/[r^*(X)]^3}{\epsilon(Y)/[r^*(Y)]^3}\right\} \tag{4}$$

and

$$T(X) = T(Y)\left[\frac{\epsilon(X)}{\epsilon(Y)}\right], \tag{5}$$

where $X$ and $Y$ are two different noble gases. In Fig. 4, we have plotted the predicted melting curves for Ne, Ar, Kr, and Xe obtained from corresponding states scaling from our newly measured He melting curve along with other experimental melting curves. It can be seen that the experimental data melting curves start to deviate from those predicted at about 20, 30, and 40 GPa for Xe, Kr, and Ar, respectively. For argon and xenon this deviation has been attributed to a gradual transition from fcc to hcp phase.[2,3,5,7] For Ne, however, the deviation is more pronounced throughout the pressure range of this study except at very low pressures (up to about 5 GPa). X-ray diffraction measurements on Ne up to 110 GPa (Ref. 23) show that it continues to remain in the parent fcc phase ruling out any phase transitions to be responsible for the discrepancy between the experimental data and the corresponding state scaling curve.

## IV. CONCLUSION

In conclusion, we have carried out melting experiments on He and Ne up to about 80 and 70 GPa, respectively, measuring temperatures using spectrometers operating in two different wavelength ranges (500–900 and 1250–1550 nm). The new experiments extend the earlier experiments by a factor of two for He and more than a factor of twelve for Ne in pressure. The present He melting curve is in good agreement with previous measurements at pressures below

2 GPa (Refs. 9 and 17) and with the data of Vos *et al.*[17] and differs significantly from the melting data of Datchi *et al.*[19] above 30 GPa. For Ne, the new melting curve does not agree with that predicted from corresponding states theory. However, the extrapolation of the new melting curve of Ne to low pressures reproduces the earlier experimental data. It seems clear that the law of the corresponding states does not well predict the behavior of the noble gases at extreme pressures. Clearly, more studies both experimental and theoretical are needed.

*goutamdev@iiserkol.ac.in


[1] A. P. Jephcoat, H.-k. Mao, L. W. Finger, D. E. Cox, R. J. Hemley, and C.-s. Zha, Phys. Rev. Lett. **59**, 2670 (1987).
[2] H. Cynn, C.-S. Yoo, B. Baer, V. Iota-Herbei, A. K. McMahan, M. Nicol, and S. Carlson, Phys. Rev. Lett. **86**, 4552 (2001).
[3] D. Errandonea, B. Schwager, R. Boehler, and M. Ross, Phys. Rev. B **65**, 214110 (2002).
[4] A. K. McMahan, Phys. Rev. B **33**, 5344 (1986).
[5] R. Boehler, M. Ross, P. Söderlind, and D. B. Boercker, Phys. Rev. Lett. **86**, 5731 (2001).
[6] M. Ross, R. Boehler, and P. Söderlind, Phys. Rev. Lett. **95**, 257801 (2005).
[7] D. Errandonea, R. Boehler, S. Japel, M. Mezouar, and L. R. Benedetti, Phys. Rev. B **73**, 092106 (2006).
[8] J. S. Dugdale and F. E. Simon, Proc. R. Soc. London, Ser. A **218**, 291 (1953).
[9] R. K. Crawford and W. B. Daniels, J. Chem. Phys. **55**, 5651 (1971).
[10] J. P. Franck, Phys. Rev. B **22**, 4315 (1980).
[11] R. L. Mills, D. H. Liebenberg, and J. C. Bronson, Phys. Rev. B **21**, 5137 (1980).
[12] P. Loubeyre, J. M. Besson, J. P. Pinceaux, and J. P. Hansen, Phys. Rev. Lett. **49**, 1172 (1982).
[13] D. Lévesque, J.-J. Weis, and M. L. Klein, Phys. Rev. Lett. **51**, 670 (1983).
[14] P. Loubeyre and J. P. Hansen, Phys. Rev. B **31**, 634 (1985).
[15] P. Loubeyre, Phys. Rev. Lett. **58**, 1857 (1987).
[16] H. K. Mao, R. J. Hemley, Y. Wu, A. P. Jephcoat, L. W. Finger, C. S. Zha, and W. A. Bassett, Phys. Rev. Lett. **60**, 2649 (1988).
[17] W. L. Vos, M. G. E. van Hinsberg, and J. A. Schouten, Phys. Rev. B **42**, 6106 (1990).
[18] P. Loubeyre, R. LeToullec, J. P. Pinceaux, H. K. Mao, J. Hu, and R. J. Hemley, Phys. Rev. Lett. **71**, 2272 (1993).
[19] F. Datchi, P. Loubeyre, and R. LeToullec, Phys. Rev. B **61**, 6535 (2000).
[20] L. Koči, R. Ahuja, A. B. Belonoshko, and B. Johansson, J. Phys.: Condens. Matter **19**, 016206 (2007).
[21] R. M. Hazen, H. K. Mo, L. W. Finger, and P. M. Bell, Year Book - Carnegie Inst. Washington **79**, 348 (1980).
[22] L. W. Finger, R. M. Hazen, G. Zou, H. K. Mao, and P. M. Bell, Appl. Phys. Lett. **39**, 892 (1981).
[23] R. J. Hemley, C. S. Zha, A. P. Jephcoat, H.-K. Mao, L. W. Finger, and D. E. Cox, Phys. Rev. B **39**, 11820 (1989).
[24] W. L. Vos, J. A. Schouten, D. A. Young, and M. Ross, J. Chem. Phys. **94**, 3835 (1991).
[25] R. Boehler and K. de Hantsetters, High Press. Res. **24**, 391 (2004).
[26] H. K. Mao, J. Xu, and P. M. Bell, J. Geophys. Res. **91**, 4673 (1986).
[27] R. Boehler, M. Ross, and D. B. Boercker, Phys. Rev. Lett. **78**, 4589 (1997).
[28] G. D. Mukherjee and R. Boehler, Phys. Rev. Lett. **99**, 225701 (2007).
[29] D. Santamaría-Pérez, M. Ross, D. Errandonea, G. D. Mukherjee, M. Mezouar, and R. Boehler, J. Chem. Phys. **130**, 124509 (2009); R. Boehler, D. Santamaría-Pérez, D. Errandonea, and M. Mezouar, J. Phys.: Conf. Ser. **121**, 022018 (2008).
[30] F. Simon and G. Glatzel, Z. Anorg. Allg. Chem. **178**, 309 (1929).
[31] V. V. Kechin, J. Phys.: Condens. Matter **7**, 531 (1995).
[32] L. Koči, R. Ahuja, and A. B. Belonoshko, Phys. Rev. B **75**, 214108 (2007).
[33] C. S. Zha, R. Boehler, D. A. Young, and M. Ross, J. Chem. Phys. **85**, 1034 (1986).
[34] A. P. Jephcoat and S. Besedin, *US-Japan Conference in Mineral Physics* (AGU, Washington D.C., 1997).